Revista Mexicana de Astronomía y Astrofísica, **61**, 49–63 (2025)

https://doi.org/10.22201/ia.01851101p.2025.61.01.04

PHOTOMETRIC LIGHT CURVE SOLUTION OF FOUR SHORT PERIOD K-SPECTRAL TYPE ECLIPSING BINARY SYSTEMS

H. Aceves[1], R. Michel[1], L. Altamirano-Dévora[1,5], F. Acerbi[2], C. Barani[3], and M. Martignoni[4]

Received March 12 2024; accepted October 8 2024

ABSTRACT

The filtered B, V, R and I light curves of four short period ($P < 0.25$d) eclipsing binary systems are presented and analysed; two having $P \approx 0.22$d, close to the short period limit for contact binaries (CBs). New ephemerides are provided. No third light was found necessary in any case, and one or more spots were introduced to account for asymmetries in the light curves. Two systems belong to the W sub-type of the W-UMa CBs and a third one to the A sub-type of the W-UMa type CBs. The last one is a semi-detached binary with a large temperature difference between the components and a low mass ratio $q = 0.191$. All components of the binaries are of the K spectral type, and the secondary of the semi-detached binary is of the M spectral type. Absolute parameters of the components were calculated using different evolutionary diagrams. Interestingly, two target have estimated total masses that are smaller than the lower mass limit known for CBs.

RESUMEN

Se analizan curvas de luz en los filtros B, V, R e I para cuatro binarias eclipsantes de periodo corto ($P < 0.25$d); dos con $P \approx 0.22$d, cercano al límite de periodo corto de binarias de contacto (CBs). Se proveen nuevas efemérides. No se encontró necesaria una tercera luz en ningún caso, y se requirieron una o dos manchas para explicar las asimetrías en las curvas de luz. Dos sistemas pertenecen al subtipo W de las W-UMa CBs y una tercera al subtipo A del tipo W-UMa. El último sistema es una binaria semi-desligada con una diferencia de temperaturas grande entre sus componentes y una razón baja de masa $q = 0.191$. Todos los componentes de las binarias son del tipo espectral K, y la secundaria de la binaria semi-desligada es del tipo espectral M. Se calculan parametros absolutos usando distintos diagramas evolutivos. Interesantemente, dos binarias presentan masas totales estimadas menores que el límite inferior en masa conocido para CBs.

Key Words: stars: fundamental parameters — stars: individual: 2MASS J09344360+4208318 (V0443 UMa, Gaia ID 814599066616791552), 2MASS J10054868+2332408, 2MASS J11393492+4128139, 2MASS J16091958+3532114 — techniques: photometric

1. INTRODUCTION

Among contact binaries (CBs) systems of spectral type K some have short periods, close to the cut-off period ($P \approx 0.22$d), according to the period-colour relation for contact binaries (Zhu et al. 2015). Moreover, as argued by Liu et al. (2023), the study of these late-type systems could provide fundamental information for understanding the nature of A and W sub-type binaries and the structure and evolution of W-UMa systems. K type binaries generally belong to the W subclass of W-UMa binaries and are in shallow contact, so they are good targets for testing the thermal relaxation oscillation (TRO) theory (Lucy 1976; Lucy & Wilson 1979; Flannery 1976; Robertson & Eggleton 1977; Yakut & Eggleton 2005 and Li et al. 2008).

The TRO theory predicts that binaries evolve in alternating cycles of contact and semi-detached

[1]Instituto de Astronomía, UNAM. Ensenada, México.
[2]Independent researcher.
[3]Independent researcher.
[4]Stazione Astronomica Betelgeuse, Magnago, Italy.
[5]FIAD-UABC, Ensenada, México.

phases with mass exchange between the components until the system reaches a high degree of contact and the binary merges into a single rapidly rotating star (Stępień 2011; Tylenda et al. 2011; Zhu et al. 2016; Liao et al. 2017).

In this work we obtain new high quality terrestrial data on four eclipsing binaries and provide photometric light curve solutions for all of them. As well, absolute elements are estimated using empirical relations from the literature. The paper is divided into nine sections. In §2 a brief description of the discovery and some published data of the systems are stated, and in §3 our new observations and ephemeris are indicated. § 4 presents our synthetic light curve solutions and in §5 estimates of absolute elements are provided. In §6 interstellar absorption parameters are given, while in §7 the stability parameter of our CBs are computed, and in §8 estimates of the energy transfer between the components of our CBs are enunciated. In §9 general remarks about our systems and final comments are presented.

2. HISTORY OF THE SYSTEMS

The system 2MASS J09344360+4208318 (hereafter J09344360), with α_{2000} = 09h 34m 43.60s and δ_{2000} = +42d 08m 31.8s, was identified as a variable star by Lohr et al. (2013) during a search in the SuperWASP (Wide Angle Search for Planets) photometric survey archive (Pollacco et al. 2006) for eclipsing binaries with very short orbital periods ($P < 20{,}000$s or ≈ 0.2315d). They found a period of 19201.57s (0.2222404d) and suggested a negative dP/dt value of -0.095 ± 0.023. The shape of the light curve and the differences in primary and secondary eclipse depths suggest that J09344360 could be a detached or semi-separated system not in thermal contact (Lohr et al. 2013). In the 82^{nd} list of variable stars, J09344360 was assigned the name V0443 UMa (Kazarovets et al. 2019). The system was observed during the low-resolution spectra survey of the Large Sky Area Multi-Object Fiber Spectroscopic Telescope (LAMOST) (Cui et al. 2012; Zhao et al. 2012) and included by Qian et al. (2020) in his catalogue of new stellar atmospheric parameters, assigning to it the EW type, the spectral type $K5$ and a temperature of 4465K.

Binary 2MASS J10054868+2332408 (hereafter J10054868), with α_{2000} = 10h 05m 48.68s and δ_{2000} = +23d 32m 40.8s, was found to be a variable of EW type with a short period of 0.2223 days by the Télescope à Action Rapide pour les Objets Transitoires, TAROT (Damerdji et al. 2007); the amplitude of variation was indicated to be 0.55 mags and the system to be of the EB/EW contact binary type. Subsequently, the system was observed in the Catalina surveys (Drake et al. 2014) and assigned a $P = 0.222324$d (19208.79s) and the W-UMa type of variability. Marsh et al. (2017) published a catalogue of 9380 W-UMa systems using the Catalina Real-Time Transient Survey Variables Sources Catalogue (Drake et al. 2014), in which our target is listed with a 0.5mags amplitude of variation and, from an empirical relationship, a temperature of $T = 4757$K for the primary component. Again, Qian et al. (2020) included J10054868 in their catalogue of new stellar atmospheric parameters, assigning to it the EW type, the period of variation $P = 0.2223243$d (19208.82s), the spectral type $K3$ and the temperature $T = 4852$K. The system was included in a long list of contact binaries selected from the Northern Catalina Sky Survey (Marsh et al. 2017) by Sun et al. (2020), who derived its relative properties using a self-developed automatic Wilson-Devinney code.

Binary 2MASS J11393492+4128139 (hereafter J11393492), with α_{2000} = 11h 39m 34.89s and δ_{2000} = +41d 28m 14.4s), was first observed by the Catalina surveys (Drake et al. 2014) with a period of $P = 0.238544$d (20610.20s) and a W-UMa type of variability. It was included in the catalogue of Marsh et al. (2017), with an amplitude of variability of 0.166 mag. and a temperature $T = 4234$K of the primary component.

Our fourth binary 2MASS J16091958+3532114 (hereafter J16091958), with α_{2000} = 16h 09m 19.58s and δ_{2000} = +35d 32m 11.4s, was reported as a variable star by the Robotic Optical Transient Search Experiment I (ROTSE-I) survey (Akerlof et al. 2000) with a period of $P = 0.247641$d and an amplitude of variation of 0.666 mag. Subsequently, the system was observed by the Catalina surveys (Drake 2014) and assigned a period of $P = 0.247632$d (21395.40s), a W-UMa type of variability, and an amplitude of variations of 0.47 mag. In the catalogue of Marsh et al. (2017), this target is listed with an amplitude of the variations of 0.483 mag and a temperature $T = 5545$K for the primary component. Also for this system, Sun et al. (2020) derived its relative properties using a self-developed automatic Wilson-Devinney code.

3. OBSERVATIONS AND NEW EPHEMERIS

Our observations follow the same general procedures used in earlier related works on binaries by our research group (Barani et al. 2022, Michel et al. 2023), and which we describe next.

Observations were done at the San Pedro Mártir Observatory (Mexico) with the 0.84-m f/15 Ritchey-

TABLE 1

LOG OF THE OBSERVATIONS

Target	UT Obs Date	ObsTime (h)	FWHM (pixels)	exp$B$ (s)	exp$V$ (s)	exp$R$ (s)	exp$I$ (s)	err$B$ (mmag)	err$V$ (mmag)	err$R$ (mmag)	err$I$ (mmag)
J09344	2022-03-21	6.44	6.7	60	40	25	25	7.6	5.6	4.5	3.5
	2023-03-25	6.23	3.9	60	40	25	25	5.8	4.5	3.6	2.8
	2023-03-28	7.11	3.6	60	40	25	25	5.8	4.5	3.6	2.8
J10054	2023-03-26	7.22	5.5	60	40	25	25	6.7	5.4	4.5	3.6
J11393	2022-03-16	4.04	4.8	80	40	30	30	22.4	14.3	8.5	5.4
	2022-04-15	3.17	3.7	40	20	15	15	24.5	14.6	9.8	5.8
	2023-03-27	9.11	3.4	60	40	25	25	11.7	9.5	7.6	4.5
J16091	2022-03-22	4.25	3.7	40	20	15	15	8.1	8.5	6.7	5.5
	2022-05-14	7.92	3.2	40	20	15	15	7.2	8.3	6.6	5.2
	2022-06-25	2.74	3.8	40	20	15	15	7.7	8.5	7.2	5.6

Chretien telescope, the Mexman filter-wheel and the *Marconi 5* CCD detector (an e2v CCD231-42 2k chip with 15×15 μm^2 pixels, gain of 2.2 e$^-$/ADU and readout noise of 3.6 e$^-$). The field of view was $9.7' \times 9.7'$ and a binning of 2×2 was employed during all the observations.

A log of the observations is shown in Table 1. FWHM is the average FWHM in binned pixels of the measured stars for the whole night. The typical differential magnitude errors (the quadratic addition of the magnitude errors of the variable and reference star) are also shown. Also the exposure times in seconds in each observed band are provided.

All the images were processed using IRAF[6] routines. Images were bias subtracted and flat field corrected before the instrumental magnitudes were computed with the standard aperture photometry method using an aperture of 1.5 times the average FWHM of the night.

The field stars were also calibrated in the $UBVRI$ system with the help of Landolt's photometric standards (Landolt 2009). Based on this information we were able to choose comparison stars with colors similar to the variables, making differential extinction corrections negligible:

1. For J09344360, star 2MASS J10381377 + 3219597: $U = 15.046, B = 15.051, V = 14.429, R = 14.054, I = 13.694$, was employed
2. For J10054868, star 2MASS J19493362 + 3141488: $U = 14.041, B = 13.008, V = 11.773, R = 11.121, I = 10.545$ was used.
3. For J11393492, star 2MASS J07334403 + 3024524 $U = 19.624, B = 18.355, V = 16.933, R = 16.079, I = 15.282$ was chosen.
4. For J16091958, star 2MASS J00000000 + 1111111 $U = 19.624, B = 18.355, V = 16.933, R = 16.079, I = 15.282$ was selected.

[6]IRAF is distributed by the National Optical Observatories, operated by the Association of Universities for Research in Astronomy, Inc., under cooperative agreement with the National Science Foundation.

From our observations we determined the apparent magnitude m_v in quadrature for J09344360 while for J10054868 we calculated the V magnitude using equations (23) of Fukugita et al. (1996). All the obtained light curves are shown in Figures 2 and 3 .

Times of minima were determined from the light curves of our binaries and new ephemeris were determined, such values are shown in Table 2. Any part of the data used here can be provided upon request.

4. SYNTHETIC LIGHT CURVE SOLUTION

To derive the parameters of the systems considered here, the photometric light curves were analysed using the latest version of the Wilson-Devinney (W-D) code (Wilson & Devinney 1971; Wilson 1990; Wilson 1994; Wilson & van Hamme 2016) using its user-friendly interface written in Python, `PyWD2015` (Güzel & Özdarcan 2020). `PyWD2015` does not change the original W-D functionality, but only provides a convenient interface for the DC and LC programs. Some useful tools in `PyWD2015` facilitate the technical aspects of the modelling process, as well as the iterative visualisation of the results.

For the light curve analysis we used the well-known procedure called "q–search". This procedure requires to set some parameters fixed in `PyWD2015` and others free (variable), with a range of fixed mass ratios ($q = m_2/m_1$). A first look at the light curves of our systems clearly shows that they exhibit continuous changes in light, suggesting the behavior of W-UMa systems and the use of `Mode 3` of the Wilson-Devinney code.

The analysis in `Mode 3` requires as fixed parameters the gravity darkening coefficients $g_1 = g_2$, set to 0.32 (Lucy 1967), the bolometric albedos

TABLE 2

TIMES OF MINIMA AND NEW EPHEMERIS

Target	HJD	Epoch	O-C	Error	Source	New ephemerid
J09344360	2454368.4008	-8848	-0.0010	0.0177	[1]	HJD2456334.7872(11) 0d.22224067(10)
	2454368.5113	-8847.5	-0.0016	0.012	[1]	
	2456334.7850	0	-0.0022	-	[2]	
	2457505.7758	5269	0.0026	0.0099	[3]	
	2457505.8912	5269.5	0.0069	0.0208	[3]	
	2459659.7290	14961	-0.0008	0.0018	[5]	
	2459659.8389	14961.5	-0.0020	0.0026	[5]	
	2460028.7609	16621.5	0.0005	0.0021	[5]	
	2460028.8708	16622	-0.0007	0.0019	[5]	
	2460031.7596	16635	-0.0011	0.0016	[5]	
	2460031.8711	16635.5	-0.0007	0.0022	[5]	
J10054868	2454118.1421	-8539.5	-0.0003	-	[1]	HJD 2456016.6796(5) 0d.2223246(1)
	2454118.2534	-8539	-0.0001	-	[1]	
	2456016.6810	0	0.0014	-	[2]	
	2457484.1350	6600.5	-0.0001	0.0107	[3]	
	2457484.2451	6601	-0.0011	0.0112	[3]	
	2460029.7656	18050.5	0.0005	0.0003	[5]	
	2460029.8760	18051	-0.0003	0.0003	[5]	
J11393492	2457307.5748	-0.5	0.0017	-	[3]	HJD 2457307.6923 (23) 0d.2385424(3)
	2457307.6906	0	-0.0017	-	[3]	
	2459654.9491	9840	0.0000	-	[5]	
	2460030.6501	11415	-0.0033	-	[5]	
	2460030.7775	11415.5	0.0049	-	[5]	
	2460030.8902	11416	-0.0017	-	[5]	
J16091958	2457506.4766	0	0.0010	0.0011	[4]	HJD 2457506.4656(27) 0d.2476461(4)
	2457548.9457	171.5	-0.0012	-	[3]	
	2459660.8713	8699.5	-0.0011	0.0020	[5]	
	2459661.0022	8700	0.0060	0.0018	[5]	
	2459713.7396	8913	-0.0052	0.0011	[5]	
	2459713.8676	8913.5	-0.0010	0.0023	[5]	
	2459755.8461	9083	0.0015	0.0011	[5]	

[1] SWASP. [2] AAVSO VSX. [3] ASAS. [4] OEJV 179. [5] This paper.

$A_1 = A_2 = 0.5$ (Ruciński 1973), and the limb darkening coefficients of the components interpolated from the square–root law tables of Claret & Bloemen (2011).

The free parameters in `Mode 3` are the temperature of the secondary component T_2, the inclination of the system i, the dimensionless potentials of the components $\Omega_{1,2}$ and the luminosity of the primary L_1. Here, the estimated temperature T_1 used for J09344360 and J10054868 were the effective temperatures obtained from LAMOST spectroscopy, which is reliable for AFGK stars (Ren et al. 2016). For J11393492 and J16091958 the average temperature for T_1 from different sources was used.

Convergence of the calculation was achieved as a contact system (`Mode 3`) for J10054868, J11393492 and J16091958. However, using `Mode 3`, we were unable to find convergence for J09344360. We therefore switched to `Mode 2`, which does not use any constraint on the potentials $\Omega_{1,2}$ (Leung & Wilson 1977), to test for a semi-detached configuration solution in `PyWD2015`. After a few iterations, the solution converged on `Mode 4` –a semi-detached configuration with star 1 filling its Roche lobe. In this mode, Ω_1 is fixed by the code to the appropriate value of the mass ratio q so that the primary component fills its Roche lobe exactly, and Ω_2 is one of the adjustable parameters. The different calculation modes offered by the W-D code are described in Wilson & van Hamme (2016).

The behavior of the q-search procedure, where the mean residual for the input data Σ is plotted against the value of the mass ratio q, is shown in Figure 1. The value of q corresponding to the minimum value of Σ was therefore included in the list of adjustable parameters and a more detailed analysis was carried out.

The presence of a third light was not found in any of the systems studied here, or its value was negligible. However, there is a further point that needs to be considered regarding J09344360 (V0443) as pointed out by the referee of this work.

The data from the Gaia mission (Gaia Collaboration et al. 2018) shows the existence of star Gaia ID 814599066616791552 (hereafter Gaia 552) only 0.7 arc seconds away from J09344360. This source

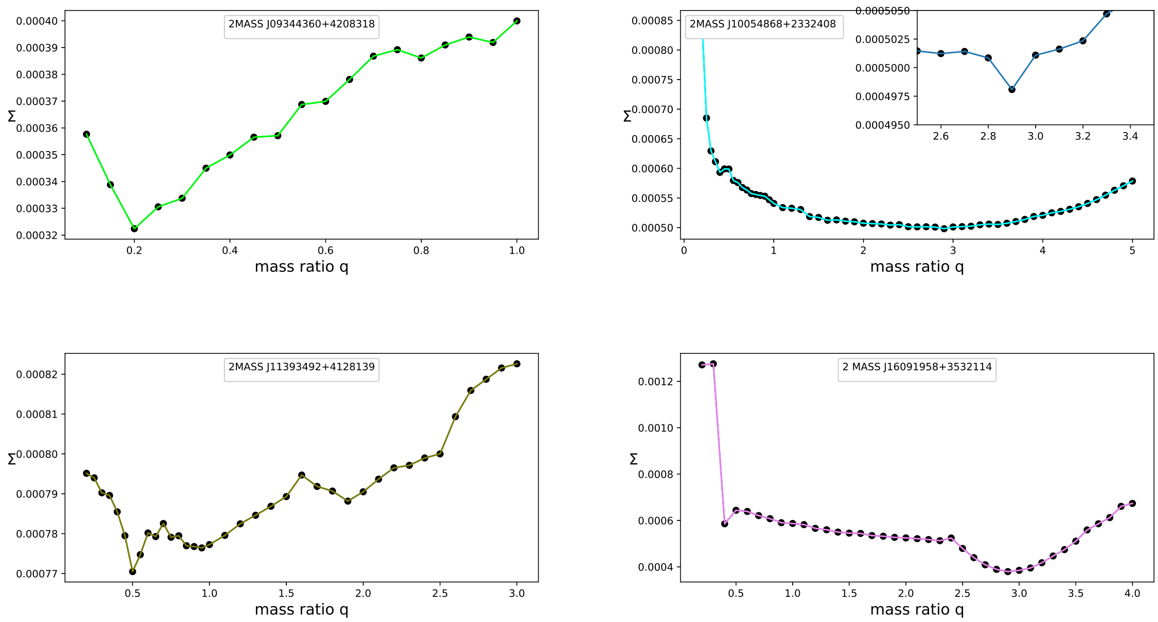

Fig. 1. Relation Σ, the mean residuals for input data, versus mass-ratio q as provided by the `PyWD2015` code. The colour figure can be viewed online.

is highlighted as non-variable and in the Gaia DR3 catalogue it is found to have a very similar magnitude and color to the average magnitude and color of J09344360. Specifically, the average G-band magnitude in Gaia is $G = 13.94$ mag for J09344360, and for Gaia 552 is $G = 14.07$ mag. Also, since the G-band time series of J09344360 is available from the Gaia DR3 catalogue, we used the Gaia light curve of J09344360 and the Gaia magnitude of Gaia 552 to evaluate the effect of this source on J09344360.

The above is necessary because the observing site of our measurements is the San Pedro Mártir Observatory (México) that has a seeing, with values measured using the DIMM, ranging from 0.48 to 0.81 arc seconds as the median value, and from 0.6 to 0.7 arc seconds as the mean value (Michel et al. 2003). All this precludes us from detecting accurate data for Gaia 552.

Now, given that it was not possible to distinguish the Gaia 552 source from J09344360 in our images, we proceeded to transform Gaia 552 luminosity into the $BVRI$ bands using the polynomials proposed by Carrasco and Bellazzini.[7]

This transformation of magnitudes allow us, by knowing the average brightness of J09344360 from Gaia measurements and our own, influenced by the luminosity of Gaia 552, to calculate the values -at each color- that are to be subtracted from our measurements to neutralize the Gaia 552-induced luminous effect. The new data obtained are used to obtain the parameters of J09344360 reported here.

In the light curves of the three contact systems the so-called O'Connell effect, different heights of the maxima, is visible (O'Connell 1951). This effect is generally attributed to the presence of a hot or cool spot on one or both components of the system. Hence in our calculations the spot parameters, co-latitude θ, longitude ψ, angular radius γ, and the temperature factor T_s/T_* have been treated as free parameters in `PyWD2015`.

Table 3 shows the results of our W-D work sessions. Note that for systems with mass ratio $q > 1$, the reciprocal value of q (q_{inv}) was used, as is generally accepted. The final fit of the observed points is shown in Figure 2 and Figure 3. Graphical representations of the systems are shown in Figure 4, using the `Binary Maker 3.0` software (Bradstreet & Steelman 2002).

5. ESTIMATES OF THE ABSOLUTE ELEMENTS

The absolute parameters of the systems presented here were estimated using the Gaia DR3 distance value (Gaia Collaboration et al. 2018).

We did not use the parallax value since all systems have a RUWE value (Renormalised Unit Weight Error) relatively high according to Lindegren

[7]`https://gea.esac.esa.int/archive/documentation/GEDR3/Data_processing/chap_cu5pho/cu5pho_sec_photSystem/cu5pho_ssec_photRelations.html`.

TABLE 3

LIGHT CURVE SOLUTIONS OF OUR FOUR SYSTEMS. ERRORS ARE THOSE OBTAINED FROM THE W-D CODE

Parameter	J09344360	J10054868	J11393492	J16091958
$i(^{\circ})$	68.994±0.683	71.982±0.212	51.644±0.806	85.688±0.406
T_1 (K)	4465(fxd)	4850(fxd)	4150(fxd)	5255(fxd)
T_2 (K)	3462±27	4528±9	3934±11	5045±5
$\Omega_1 = \Omega_2$		6.380±0.030	2.913±0.022	6.413±0.006
Ω_1	2.221(fxd)			
Ω_2	2.331±0.045			
q	0.191±0.009	2.923±0.022	0.510±0.009	2.896±0.001
$1/q$		0.342		0.345
f	0%	21.70%	0.45%	10.50%
f_2	0.051%			
L_{1B}	0.993±0.003	0.372±0.004	0.635±0.043	0.322±0.001
L_{1V}	0.987±0.003	0.348±0.004	0.636±0.037	0.310±0.001
L_{1R}	0.975±0.003	0.328±0.003	0.634±0.032	0.303±0.001
L_{1I}	0.953±0.003	0.315±0.002	0.638±0.024	0.294±0.001
L_{2B}	0.010±0.001	0.577±0.008	0.023±0.001	0.640±0.010
L_{2V}	0.016±0.001	0.594±0.010	0.024±0.001	0.653±0.011
L_{2R}	0.024±0.001	0.609±0.001	0.026±0.001	0.670±0.014
L_{2I}	0.040±0.001	0.628±0.014	0.028±0.001	0.669±0.015
L_{3BVRI}	0	0	0	0
Primary				
r(pole)	0.490±0.004	0.281±0.001	0.411±0.002	0.276±0.001
r(side)	0.534±0.005	0.294±0.001	0.436±0.003	0.288±0.001
r(back)	0.556±0.004	0.334±0.001	0.465±0.003	0.324±0.001
Secondary				
r(pole)	0.202±0.019	0.454±0.002	0.304±0.007	0.449±0.001
r(side)	0.208±0.021	0.489±0.003	0.318±0.008	0.482±0.001
r(back)	0.224±0.029	0.518±0.005	0.351±0.013	0.510±0.001
Residual	0.00032406	0.00050008	0.00076165	0.00037905
Lat_{spot}		10°3.4±1.3	30°.3±1.1	51°.7±1.2
$Long_{spot}$		120°.7±1.1	110°.5±1.6	72°.1±0.9
Radius		20°.8±0.45	28°.2±0.93	20°.5±0.66
T/F		0.97±0.06	0.87±0.09	1.23±0.10
Component		1	1	1
Lat_{spot}		90°.6±1.2		
$Long_{spot}$		181°.1±1.2		
Radius		17°.3±0.51		
T/F		0.94±0.03		
Component		2		

(2018); see Table 5. In particular J09344360 and J11393492 have a RUWE value of ≈ 2.

For J09344360 the distance value was missing in the Gaia DR3 catalog and therefore the absolute parameters were estimated using the following relations:

(a) Period-Mass ($P-M_1$) relation obtained from the absolute parameter estimates of 118 systems using the parallax method from Gaia DR3 (Poro et al. 2022),

$$M_1 = (2.924 \pm 0.075)P + (0.147 \pm 0.029)\ .$$

(b) Orbital period-semimajor axis (P-a) relation as suggested by Poro et al. (2024), obtained from the study of 414 contact systems with $P < 0.7$ days from Latković et al. (2021),

$$a = 5.914^{+0.272}_{-0.298}\, P + 0.372^{+0.113}_{-0.114}\ .$$

Subsequently, knowing the mass ratio q, the fractional radii $r_{1,2}$ and the temperatures of the components of J09344360, the values of the absolute radii and luminosities $R_{1,2}$ and $L_{1,2}$ were obtained from the well-known formula $R_{1,2} = a \times r_{mean}$ and the Stefan-Boltzmann law.

For the other systems knowing the distance we calculated: the visual absolute magnitude M_v, the bolometric magnitude M_{bol}, the total luminosity L_{tot} and the individual luminosities $L_{1,2}$ using the following equations:

$$M_v = m_v - 5\log d + 5 - A_v\ ,$$

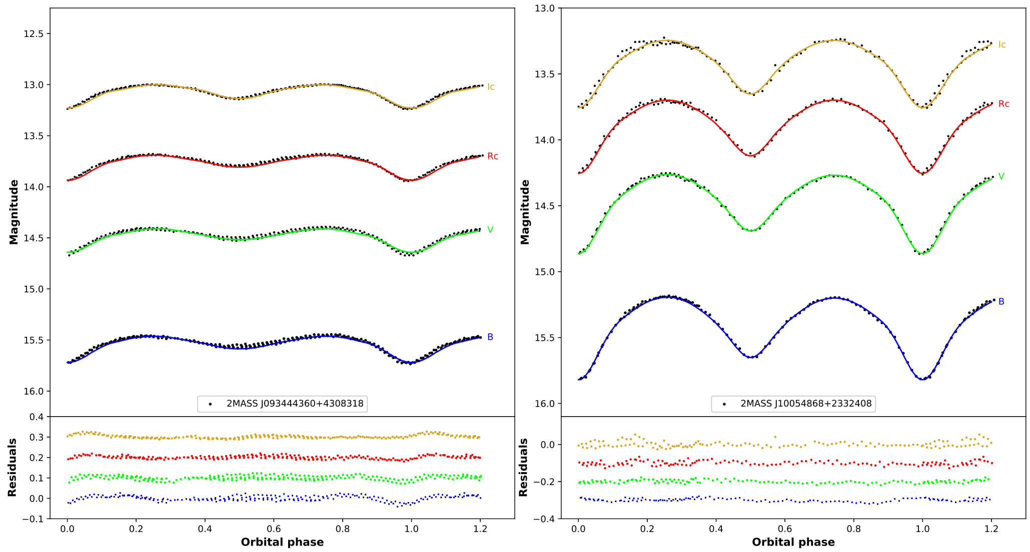

Fig. 2. CCD light curves of 2MASS J09344360+4208318 and 2MASS J10054868+2332408. Points are the original CCD observations and lines are the theoretical fits with the surface spot/s contribution. The residuals are shown at the bottom of each panel, arbitrarily shifted for clarity. The colour figure can be viewed online.

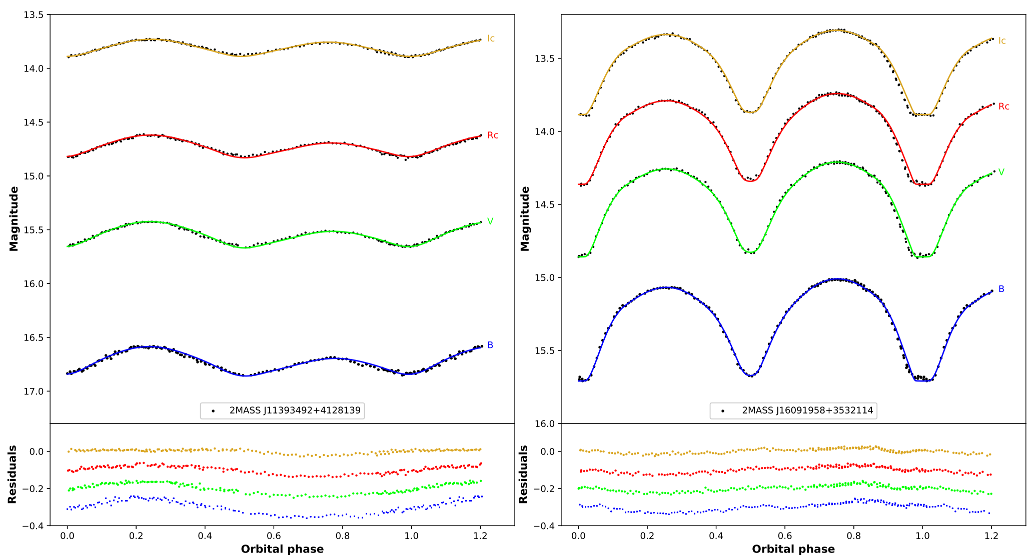

Fig. 3. The same of Figure 2 but for 2MASS J11393492+4128139 and 2MASS J16091958+3532114. The colour figure can be viewed online.

where m_v is the V magnitude, d the distance in parsec and A_v the interstellar absorption; $M_{bol} = M_v + BC$, where BC is the star's bolometric correction as interpolated from the Pecaut & Mamajek (2013) tables;

$$\log(L_{tot}/L_{\odot}) = 0.4 \times (4.74 - M_{bol})\,;$$

$L_1 = L_{tot}/c$, $c = L_{2V}/L_{1V}$, and $L_2 = L_{tot} - L_1$.

The temperatures of the first and second components of the systems are known, so we obtained their radii $R_{1,2}$, the semi-axis a, and the total mass of the systems from Kepler's third law as follows:

$$R_{1,2}[\mathrm{R}_{\odot}] = L_{1,2}[\mathrm{L}_{\odot}]^{1/2}/T_{1,2}[\mathrm{T}_{\odot}]^2\ ,$$

where $T_{\odot} = 5771.8$K, and

$$a = R_1/r_{1mean}\,;$$

$$M_{tot} = 0.0134\,(a^3/P^2)\,.$$

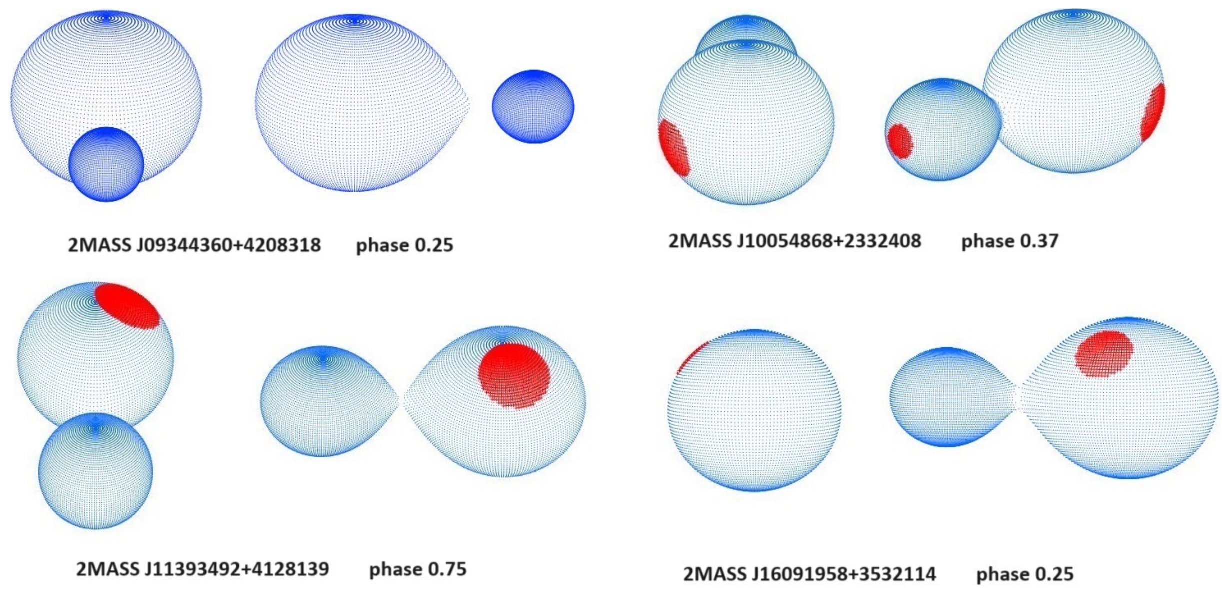

Fig. 4. The 3D view of the stars. Left at the primary minimum, right with the spot/s visible. The colour figure can be viewed online.

TABLE 4

ABSOLUTE ELEMENTS VALUES FOR ALL THE SYSTEMS

Target	$M_1(\mathrm{M}_\odot)$	$M_2(\mathrm{M}_\odot)$	$R_1(\mathrm{R}_\odot)$	$R_2(\mathrm{R}_\odot)$	$L_1(\mathrm{L}_\odot)$	$L_2(\mathrm{L}_\odot)$	$M_{tot}(\mathrm{M}_\odot)$
J09344360	0.797±0.003	0.153±0.008	0.888±0.011	0.356±0.039	0.283±0.007	0.016±0.004	0.949
J10054868	1.125±0.190	0.385±0.089	0.840±0.044	0.561±0.016	0.267±0.026	0.157±0.009	1.510
J11393492	0.418±0.190	0.213±0.100	0.868±0.075	0.189±0.070	0.202±0.035	0.008±0.071	0.631
J16091958	0.659±0.090	0.228±0.032	0.758±0.011	0.481±0.026	0.335±0.007	0.159±0.022	0.887
	J_0	$\log J_0$	J_{lim}	$\log J_{lim}$	Spec. type	$\log \rho_1(\mathrm{gr/cm^3})$	$\log \rho_2(\mathrm{gr/cm^3})$
J09344360	9.29^{50}	50.97	2.47^{51}	50.97	K5 + M3	0.34	0.81
J10054868	2.74^{51}	51.44	4.26^{51}	51.63	K3 + K4-5	0.54	0.39
J11393492	7.74^{50}	50.89	1.01^{51}	51.00	K7 + K9	0.42	0.63
J16091958	1.18^{51}	51.07	1.70^{51}	51.23	K0 + K2	0.48	0.31

Note: Spectral types are according to Pecaut & Mamajek (2013).

Using the value of the mass ratio from the Wilson-Devinney analysis, we obtained the masses M_1 and M_2, and therefore all the physical parameters of the systems under study, whose values are shown in Table 4.

6. INTERSTELLAR ABSORPTION

For the calculation of A_v we used the NASA & IPAC Galactic Dust Reddening and Extinction maps[8] obtaining the total interstellar absorption in the photometric V band value of the color excess $E\infty(B-V)$ from Schlafly & Finkbeiner (2011) and Schlegel et al. (1998).

[8]The NASA&IPAC Extragalactic Database (NED) is funded by the National Aeronautics and Space Administration and operated by the California Institute of Technology.

Subsequently the value of the total interstellar absorption in the V band up to the distance d was calculated via the well known Bahcall & Soneira (1980) relation:

$$A_d(b) = A_\infty(b)[1-\exp(-d\sin b/H)]\,, \tag{1}$$

where H is the scale height for the interstellar dust, which is adopted to be 125 pc (Marshall et al. 2006); values are shown in Table 5.

7. STABILITY PARAMETER

The Flannery (1976) stability parameter $\Im$ for mass exchange in a contact binary system can be defined as follows:

$$\Im = \ln\left[\frac{R_p(0.38+0.2\log q)}{R_s(0.38-0.2\log q)}\right]\,, \tag{2}$$

TABLE 5

TOTAL INTERSTELLAR ABSORPTION

Target	b	d	RUWE	A_v
J09344360	47.506	365.61	1.990	0.036
J10054868	52.570	399.60	1.002	0.090
J11393492	69.443	411.45	2.037	0.057
J16091958	47.361	540.02	0.983	0.055

where R_p is the radius of the primary and R_s is the radius of the secondary.

If $\Im = 0$, there is no mass transfer; if $\Im > 0$, an unbalanced pressure gradient will force gas from the primary to the secondary, and vice versa if $\Im < 0$.

In the cases studied here we get $\Im = 0.74$ for J09344360 and $\Im = 1.21$ for J11393492, so there is mass transfer from the primary to the secondary. The opposite ($\Im < 0$) is true for J10054868 and J16091958 where we get $\Im = -0.90$ and -0.95 respectively.

8. ENERGY TRANSFER IN OUR BINARIES

One of the characteristics of the secondary components of contact binary systems is that they are brighter and larger than their zero-age main sequence (ZAMS) counterparts (Struve 1948).

In fact, as far as our target systems are concerned we show their radii and luminosity data in Table 6, in comparison to their main sequence analog and, as observed, the secondaries display such behavior.

According to the studies of Wang (1994), Csizmadia & Klagyivik (2004) and Jiang et al. (2009), we can estimate the energy transfer parameter β and the luminosity transfer from primary to secondary ΔL as, respectively:

$$\beta = \frac{L_{1,obs}}{L_{1,ZAMS}} = \frac{1 + q^{4.6}}{1 + q^{0.92} X (T_2/T_1)^4}, \qquad (3)$$

and

$$\Delta L = (1 - \beta) X L_1 \,, \qquad (4)$$

where X is the relative temperature difference parameter $(T_1 - T_2)/T_1$.

Therefore the percentage of the intrinsic luminosity of the primary that is transferred to the secondary during the energy transfer process can be estimated with the previous relationships in equations (3) and (4).

Furthermore, we can calculate the effects of the energy transfer on the secondary, for example, the increase in luminosity ΔL_2 (Yang & Liu 2001) and the decrease in radius R_2 to become a main sequence star, in terms of the logarithm of $dR_2/R_{2,ZAMS}$ (Jiang et al. 2009). The estimates of these quantities are displayed in Table 7.

9. DETAILS ON THE SYSTEMS AND FINAL REMARKS

9.1. *Common Features*

The common features of our systems can be summarised in a few relevant points:

(1) The four systems studied here, although with some differences among them that will be explained later, belong to the late spectral type K and, with their short periods, are good targets for testing the thermal relaxation oscillation (TRO) theory (Lucy 1976; Lucy & Wilson 1979; Flannery 1976; Robertson & Eggleton 1977; Yakut & Eggleton 2005 and Li et al. 2008), and are of great interest for the study of the structure and evolution of eclipsing binaries (Acerbi et al. 2022). The TRO model predicts that binaries evolve in a cycle around the marginal contact state, oscillating between contact-semidetached-contact states and exhibiting alternate EW and EB light curves (Zhu et al. 2010).

(2) In addition, the three systems close to the short period limit of 0.22 days are ultra-short period binaries (USPBs) (Rucinski 1992; Rucinski 2007). These binaries are important objects for studying the period cut-off phenomenon (Liu et al. 2014; Li et al. 2019). Although many studies have been conducted on the period distribution of close binaries, the values of the period limit and the period cut-off are still open questions. However, thanks to the use of data from several photometric surveys, Qian et al. (2020) recently proposed a new period cut-off value of 0.15 days and concluded that the maximum of the period distribution of close binaries is about 0.31 days. The same conclusion was reached by Latković et al. (2021) who found the maximum of the period distribution to be close to 0.3 days.

(3) The low degree of contact is another common feature of the four binary systems studied here, which is a well-known feature of K-type systems.

9.2. *J09344360*

This binary is a short-period ($P \approx 0.22$d) formally semi-detached system (Figure 5, left), as also argued by Lohr et al. (2013), in which the primary component fills its Roche lobe while the secondary is a little inside it ($f = 0.051$).

The stability parameter ($\Im = 0.74$) suggests that there is currently mass transfer between the components.

TABLE 6

SECONDARIES OF CBs AND THEIR ZAMS COUNTERPARTS

Target	$R_2(R_\odot)$	$R_{2,ZAMS}(R_\odot)$	$L_2(L_\odot)$	$L_{2,ZAMS}(L_\odot)$
J10054868	0.840	0.381	0.267	0.018
J11393492	0.189	0.225	0.008	0.004
J16091958	0.758	0.239	0.267	0.005

TABLE 7

TRANSFER ENERGY PARAMETERS

Target	β	ΔL	ΔL_2	$\log \mathrm{d}R_2/R_{2,ZAMS}$
J10054868	0.785	0.034	0.245	-0.152
J11393492	0.729	0.055	0.006	-0.374
J16091958	0.764	0.038	0.332	-0.156

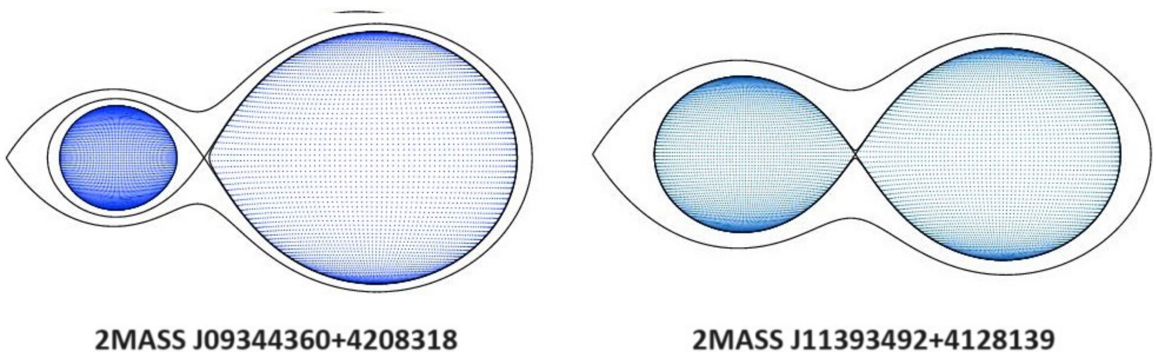

Fig. 5. The configuration of the components of 2MASS J09344360+4208318 (V0443 UMa) and 2MASS J11393492+4128139 in the orbital plane is shown. The colour figure can be viewed online.

The later spectral type of the components ($K5 + M3$) is indicative of an old formed system that has probably experienced more than one TRO cycle and is now in a slightly semi-detached state far from thermal stability ($\Delta T \approx 1000$K).

With the current extreme mass ratio of $q = 0.191$, it is likely that this system may be at the beginning of a new phase of contact binary evolution, as suggested by its position in the heat diagram of Figure 7 near the outer edge of the lower (red) boundary.

The location of the secondary component in the $\log M - \log L$ diagram (Figure 6) and the total mass of the system ($M_{tot} = 0.95$M$_\odot$), slightly below the lower mass limit of 1.0-1.2M$_\odot$ for the known contact binaries Stępień (2006), suggests that it has lost mass during the TRO cycles and may imply a later evolutionary stage.

9.3. *J10054868, J11393492 and J16091958*

All three systems are contact binaries with short periods ($P \approx 0.22$-0.25 d) and in which the temperature of the components suggests a spectral type K.

J11393492 is an A-subtype contact system while J10054868 and J16091958 are W-subtype contact systems. It is worth noticing that it is somewhat strange to find a spectral K type in A-subtype contact systems. Late spectral type systems generally belong to the W-subtype of W UMa contact binaries, although it is possible to find exceptions to this in the literature, as ES Cep (Zhu et al. 2014), 2MASS J11201034-2201340 (Hu et al. 2016), AP UMi (Awadalla et al. 2016), NSV 395 (Samec et al. 2016), ROTSE J135349.8+305205 and 1SWASP J150957.5-115308 (Barani et al. 2022). The mass ratio of J11393492 is $q = 0.51$ and from the W-D analysis a shallow filling value of $f = 4.5$ (Figure 5,

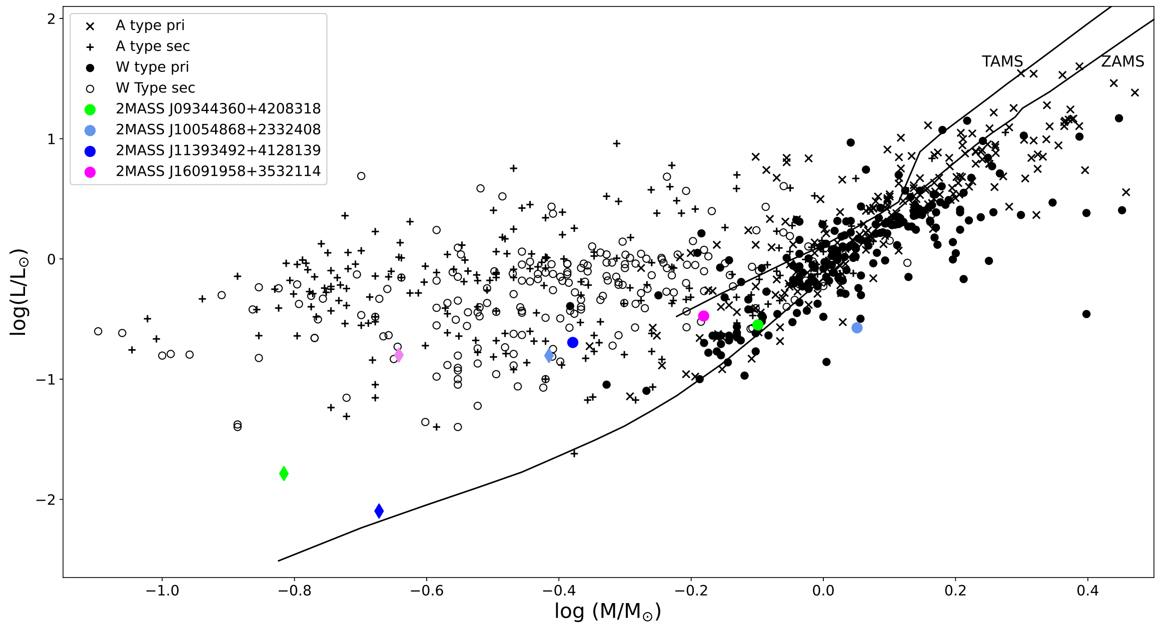

Fig. 6. Location of the components of our systems on the logarithmic Mass-Luminosity diagram. The primaries are marked with circles and the secondaries with diamonds. The sample of W UMa type systems was obtained from a compilation of Latković et al. (2021). Zero Age Main Sequence (ZAMS) and Terminal Age Main Sequence (TAMS) are taken from Girardi et al. (2000) for the solar chemical composition. The colour figure can be viewed online.

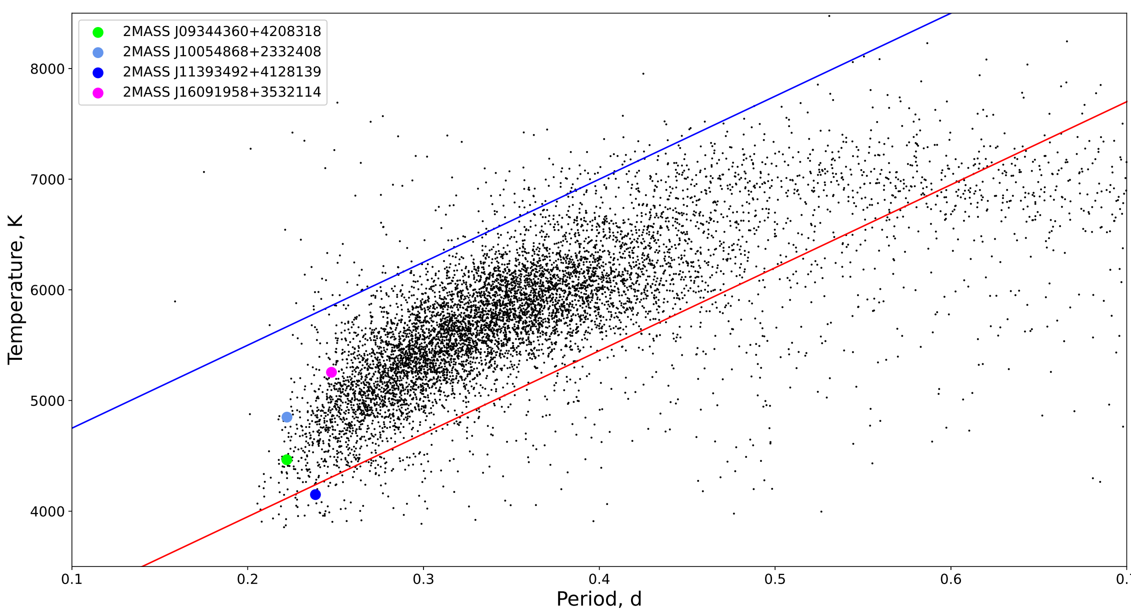

Fig. 7. Correlation between orbital period and temperature based on parameters of 8510 contact binaries from Qian et al. (2020). The red and blue lines are the boundaries of normal EWs. Systems near the red border are marginal contact systems, while those close to the blue border are deep contact ones. The colour figure can be viewed online.

right) was found, despite that it is in good thermal contact with only $\Delta T = 216$K. A cool spot, generally associated with magnetic activity such as solar magnetic spots (Mullan 1975), was added to the primary component to account for the asymmetries in its light curve (Figure 4).

The stability parameter is positive ($\Im = +1.21$), so we currently have a mass transfer from the primary to the secondary component of the system.

J10054868 and J16091958 show common features that are the good thermal contact between their components, the shallow fill-out and the presence of spot(s) (Table 3). While for J16091958 the hot spot is produced by the impact of mass transferred from the secondary to the primary component, which is supported by the value of the Flannery parameter ($\Im = -0.90$), for J10054868 a cool spot, possibly caused by magnetic activity, was required on the component to account for the discrepancies in the light curve.

The relative properties of both the systems were derived by Sun et al. (2020) using a self-developed automatic Wilson-Devinney code. With respect to J10054868, the more obvious difference between their solution and ours is that we obtain a W-subtype, whereas Sun et al. (2020) obtain an A- subtype W UMa.

It is however known (e.g. van Hamme (1982), Lapasset & Claria (1986)) that sometimes both A and W configurations can reproduce well the photometric light curve, and the right choice between the two solutions can be obtained only having a spectral mass ratio.

For our two systems, after starting the two solutions with very similar temperatures of the primary component, we obtained encouraging similar results with those of Sun et al. (2020) with only minor differences in the mass ratio q of about 1/3, theirs smaller than ours. A luminosity $L_{1\odot}$ for J10054868 twice as large was obtained here; they obtain a luminosity for J16091958 1/3 larger than our result.

It is also necessary to note that during their solutions Sun et al. (2020), did not consider the effect of starspots, while we have found two cool spots on the components for J10054868 and one cool spot on the primary component of J16091958. This is probably the reason of such discrepancy.

Figure 6 shows the positions of the components of our systems in the $\log M - \log L$ diagram where they are located with other W UMa systems from the Latković et al. (2021). The ZAMS and TAMS lines are calculated from Girardi et al. (2000).

The position of the components of J10054868 is among the other primaries and secondaries of the sample, while the primary components of J11393492 and J16091958 are near the TAMS, implying that they have evolved away from the main sequence. These results are due to the mass and energy exchange between the binary components and their internal evolutionary transformations. The secondary components deviate significantly from ZAMS, like the majority of the secondaries of other W UMa systems, meaning that they are little evolved (J11393492) or evolved (J16091958) stars and this may be due to the energy transfer from the more massive component to the less massive one during their evolutionary process (Li et al. 2008).

From the heat map shown in Figure 7 it is possible to observe that both current systems are located inside the boundaries for normal EW systems, with similar positions between the red and blue lines that are the boundaries of the normal EW systems. The position of J11393492 in this Figure 7 is slightly below the red line, and in the $\log M - \log J_0$ (Figure 8) is close to the line that separates the contact from the detached region. The latter suggests that the system, with its filling factor close to zero and the almost equal temperature of its components, is either at the end or at the beginning of the contact phase, as predicted by the TRO theory. The small mass ratios, $q \approx 0.34$ for both J10054868 and J16091958, their low fill-out value, 21.7% and 10.5% respectively, the almost equal temperature of the components, and their position in the contact region of the $\log M - \log J_0$ diagram (Figure 8) suggest that they are approaching the final evolutionary stage of contact binaries. The total estimated masses for J11393492 $M_{tot} = 0.63\mathrm{M}_\odot$ and of J16091958 $M_{tot} = 0.89\mathrm{M}_\odot$ are below the lower mass limit of $1.0 - 1.2\mathrm{M}_\odot$ for known contact binaries (Stępień 2006).

This work has made use of data from the European Space Agency (ESA) mission Gaia,[9] and processed by the Gaia Data Processing and Analysis Consortium (DPAC).[10] Our new observations were carried out at the Observatorio Astronómico Nacional on the Sierra San Pedro Mártir (OAN-SPM), Baja California, México, which is operated by the Universidad Nacional Autónoma de México (UNAM). This work has made use of data from the International Variable Star Index (VSX) database (operated at AAVSO Cambridge, Massachusetts, USA), as well as of the AAVSO Photometric All-Sky Survey (APASS) funded by the Robert Martin Ayers Sci-ences Fund. Also, use has been made of the VizieR catalogue access tool, the SIMBAD database, operated at CDS, Strasbourg, France. The original description of the VizieR service was published in

[9] https://www.cosmos.esa.int/gaia.

[10] https://www.cosmos.esa.int/web/gaia/dpac/consortium.

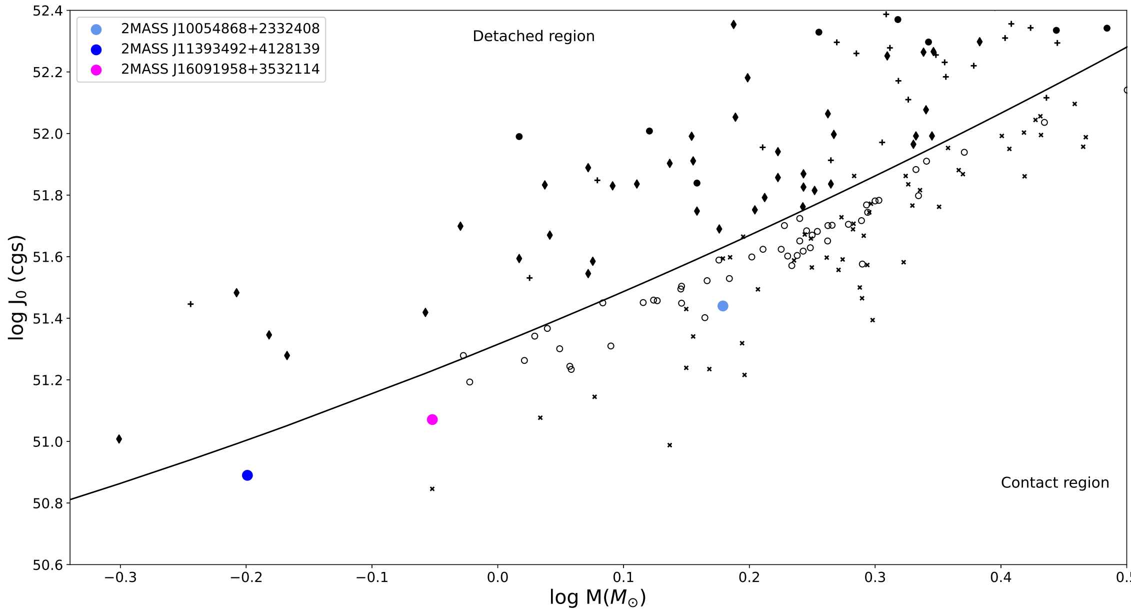

Fig. 8. Position of the three contact systems in the $\log M_\odot - \log J_0$ diagram. Symbols are described in Figure 1 of the original paper of Eker et al. (2006). The colour figure can be viewed online.

A&AS 143, 23. Use of the NASA/IPAC Extragalactic Database (NED), which is founded by the National Aeronautics and Space Administratrion and operated by the California Institute of Technology, has been made. We would like to thank the anonymous referee for her/his useful comments which have improved the quality of this paper, and in particular for calling our attention to the presence of a companion to J09344360, as detected by GAIA, and suggestions on how to consider such effect. We also thank Dr. Gisella Clementini (INAF, Bologna) for her helpful suggestions and clarifications regarding GAIA observations on J09344360.

REFERENCES

Acerbi, F., Barani, C., & Popov, V. 2022, NewA, 97, 101873, https://doi.org/10.1016/j.newast.2022.101873

Akerlof, C., Amrose, S., Balsano, R., et al. 2000, AJ, 119, 1901, https://doi.org/10.1086/301321

Awadalla, N. S., Hanna, M. A., Ismail, M. N., et al. 2016, JKAS, 49, 65, https://doi.org/10.5303/JKAS.2016.49.3.065

Bahcall, J. N. & Soneira, R. M. 1980, ApJS, 44, 73, https://doi.org/10.1086/190685

Barani, C., Martignoni, M., Michel, R., Acerbi F., Aceves H., Popov V. 2022, RMxAA, 58, 237, https://doi.org/10.22201/ia.01851101p.2022.58.02.06

Bradstreet, D. H. & Steelman, D. P. 2002, AAS, 201, 1124

Claret, A. & Bloemen, S. 2011, A&A, 529, 75, https://doi.org/10.1051/0004-6361/201116451

Cui, X.-Q., Zhao, Y.-H., Chu, Y.-Q., et al. 2012, RAA, 12, 1197, https://doi.org/10.1088/1674-4527/12/9/003

Csizmadia, S. & Klagyivik, P. 2004, A&A, 426, 1001, https://doi.org/10.1051/0004-6361:20040430

Damerdji, Y., Klotz, A., & Boër, M. 2007, AJ, 133, 1470, https://doi.org/10.1086/511747

Drake, A. J., Graham, M. J., Djorgovski, S. G., et al. 2014, ApJS, 213, 9, https://doi.org/10.1088/0067-0049/213/1/9

Flannery, B. P. 1976, ApJ, 205, 217, https://doi.org/10.1086/154266

Fukugita, M., Ichikawa, T., Gunn, J. E., et al. 1996, AJ, 111, 1748, https://doi.org/10.1086/117915

Gaia Collaboration, Brown, A. G. A., Vallenari, A., et al. 2018, A&A, 616, 1, https://doi.org/10.1051/0004-6361/201833051

Girardi, L., Bressan, A., Bertelli, G., et al. 2000, A&AS, 141, 371, https://doi.org/10.1051/aas:2000126

Güzel, O. & Özdarcan, O. 2020, Contributions of the Astronomical Observatory Skalnate Pleso, 50, 535, https://doi.org/10.31577/caosp.2020.50.2.535

Hu, C.-P., Yang, T.-C., Chou, Y., et al. 2016, AJ, 151, 170, https://doi.org/10.3847/0004-6256/151/6/170

Jiang, D., Han, Z., Jiang, T., et al. 2009, MNRAS, 396, 2176, https://doi.org/10.1111/j.1365-2966.2009.14852.x

Kazarovets, E. V., Samus, N. N., Durlevich, O. V., et al. 2019, IBVS, 6261, 1, https://doi.org/10.22444/IBVS.6261
Landolt, A. U. 2009, AJ, 137, 4186, https://doi.org/10.1088/0004-6256/137/5/4186
Lapasset, E. & Claria, J. J. 1986, A&Ap, 161, 264
Latković, O., Čeki, A., & Lazarević, S. 2021, ApJS, 254, 10, https://doi.org/10.3847/1538-4365/abeb23
Leung, K.-C. & Wilson, R. E. 1977, ApJ, 211, 853, https://doi.org/10.1086/154994
Li, L., Zhang, F., Han, Z., et al. 2008, MNRAS, 387, 97, https://doi.org/10.1111/j.1365-2966.2008.12736.x
Li, K., Xia, Q.-Q., Michel, R., et al. 2019, MNRAS, 485, 4588, https://doi.org/10.1093/mnras/stz715
Liao, W.-P., Qian, S.-B., Soonthornthum, B., et al. 2017, PASP, 129, 124204, https://doi.org/10.1088/1538-3873/aa8ded
Lindgren, L., 2018, Re-normalising the astrometric chi-square in Gaia DR2 note GAIA-C3-TN-LU-LL- 124, Gaia DPAC
Liu, N.-P., Qian, S.-B., Soonthornthum, B., et al. 2014, AJ, 147, 41, https://doi.org/10.1088/0004-6256/147/2/41
Liu, N.-P., Qian, S.-B., Liao, W.-P., et al. 2023, AJ, 165, 259, https://doi.org/10.3847/1538-3881/acd04e
Lohr, M. E., Norton, A. J., Kolb, U. C., et al. 2013, A&A, 549, A86, https://doi.org/10.1051/0004-6361/201220562
Lucy, L. B. 1967,ZAp, 65, 89
Lucy, L. B. 1976, ApJ, 205, 208, https://doi.org/10.1086/154265
Lucy, L. B. & Wilson, R. E. 1979, ApJ, 231, 502, https://doi.org/10.1086/157212
Marsh, F. M., Prince, T. A., Mahabal, A. A., et al. 2017, MNRAS, 465, 4678, https://doi.org/10.1093/mnras/stw2110
Marshall, D. J., Robin, A. C., Reylé, C., et al. 2006, A&A, 453, 635, https://doi.org/10.1051/0004-6361:20053842
Michel, R., Echevarría, J., Costero, R., et al. 2003, RMxAA, 39, 291
Michel, R., Barani, C., Martignoni, M., et al. 2023, RMxAA, 59, 123, https://doi.org/10.22201/ia.01851101p.2023.59.01.09
Mullan, D. J. 1975, ApJ, 198, 563, https://doi.org/10.1086/153635
O'Connell, D. J. K. 1951, Publications of the Riverview College Observatory, 2, 85
Pecaut, M. J. & Mamajek, E. E. 2013, ApJS, 208, 9, https://doi.org/10.1088/0067-0049/208/1/9
Pollacco, D. L., Skillen, I., Collier Cameron, A., et al. 2006, PASP, 118, 1407, https://doi.org/10.1086/508556
Poro, A., Sarabi, S., Zamanpour, S., et al. 2022, MNRAS, 510, 5315, https://doi.org/10.1093/mnras/stab3775
Poro, A., Tanriver, M., Michel, R., et al. 2024, PASP, 136, 024201, https://doi.org/10.1088/1538-3873/ad1ed3
Qian, S.-B., Zhu, L.-Y., Liu, L., et al. 2020, RAA, 20, 163, https://doi.org/10.1088/1674-4527/20/10/163
Ren, A., Fu, J., De Cat, P., et al. 2016, ApJS, 225, 28, https://doi.org/10.3847/0067-0049/225/2/28
Robertson, J. A. & Eggleton, P. P. 1977, MNRAS, 179, 359, https://doi.org/10.1093/mnras/179.3.359
Ruciński, S. M. 1973, Acta Astron., 23, 79
Rucinski, S. M. 1992, AJ, 103, 960, https://doi.org/10.1086/116118
Rucinski, S. M. 2007, MNRAS, 382, 393, https://doi.org/10.1111/j.1365-2966.2007.12377.x
Samec, R. G., Clark, J., Maloney, D., et al. 2016, JAAVSO, 44, 101
Schlafly, E. F. & Finkbeiner, D. P. 2011, ApJ, 737, 103, https://doi.org/10.1088/0004-637X/737/2/103
Schlegel, D. J., Finkbeiner, D. P., & Davis, M. 1998, ApJ, 500, 525, https://doi.org/10.1086/305772
Stępień, K. 2006, Acta Astron., 56, 347, https://doi.org/10.48550/arXiv.astro-ph/0701529
Stępień, K. 2011, Acta Astron., 61, 139, https://doi.org/10.48550/arXiv.1105.2645
Struve, O. 1948, AnAp, 11, 117
Sun, W., Chen, X., Deng, L., et al. 2020, ApJS, 247, 50, https://doi.org/10.3847/1538-4365/ab7894
Tylenda, R., Hajduk, M., Kamiński, T., et al. 2011, A&A, 528, A114, https://doi.org/10.1051/0004-6361/201016221
van Hamme, W. 1982, A&Ap,, 105, 389
Wang, J.-M. 1994, ApJ, 434, 277, https://doi.org/10.1086/174725
Wilson, R. E. & Devinney, E. J. 1971, ApJ, 166, 605, https://doi.org/10.1086/150986
Wilson, R. E. 1990, ApJ, 356, 613, https://doi.org/10.1086/168867
Wilson, R. E. 1994, PASP, 106, 921, https://doi.org/10.1086/133464
Wilson, R. E. & van Hamme, W., 2016, Computing Binary Stars Observables. ftp.astro.u.edu, directory pub/wilson/lcdc2015
Yakut, K. & Eggleton, P. P. 2005, ApJ, 629, 1055, https://doi.org/10.1086/431300
Yang, Y. & Liu, Q. 2001, AJ, 122, 425, https://doi.org/10.1086/321110
Zhao, G., Zhao, Y.-H., Chu, Y.-Q., et al. 2012, RAA, 12, 723, https://doi.org/10.1088/1674-4527/12/7/002
Zhang, X.-D. & Qian, S.-B. 2020, MNRAS, 497, 3493, https://doi.org/10.1093/mnras/staa2166
Zhu, L., Qian, S.-B., Mikulášek, Z., et al. 2010, AJ, 140, 215, https://doi.org/10.1088/0004-6256/140/1/215
Zhu, L. Y., Qian, S. B., Soonthornthum, B., et al. 2014, AJ, 147, 42, https://doi.org/10.1088/0004-6256/147/2/42

Zhu, L.-Y., Qian, S.-B., Jiang, L.-Q., et al. 2015, ASPC 496, Living Together: Planets, Host Stars and Binaries, ed. S. M. Rucinski, G. Torres, and M. Zejda, (San Francisco, CA: ASPC), 200
Zhu, L.-Y., Zhao, E.-G., & Zhou, X. 2016, RAA, 16, 68, https://doi.org/10.1088/1674-4527/16/4/068

F. Acerbi: Via Zoncada 51, Codogno, LO, 26845, Italy (acerbifr@tin.it).
H. Aceves: Instituto de Astronomía, UNAM. A.P. 877, 22800 Ensenada, BC, México (aceves@astro.unam.mx).
L. Altamirano-Dévora: Facultad de Ingeniería, Arquitectura y Diseño, UABC, Ctra. Tij-Ens 3917, 22860 Ensenada, BC, México (lili@astro.unam.mx).
C. Barani: Via Verdi 25, Codogno, LO, 26845, Italy (carlobarani.cb@gmail.com).
M. Martignoni: Via Don G. Minzoni 26/D, Magnago, MI, 20020, Italy (massimiliano.martignoni@outlook.it).
R. Michel: Instituto de Astronomía, UNAM. A.P. 877, 22800 Ensenada, BC, México (rmm@astro.unam.mx).